Investigation of the Impact of Seismic Noise on LIGO Interferometer Performance

Rachel Brodsky[1], Thomas Massinger[2], Jessica McIver[2]

September 1, 2017

1. The University of Pennsylvania
2. The California Institute of Technology

1 Introduction

Einstein's Theory of General Relativity predicts that the acceleration of asymmetric matter, such as binary black hole and binary neutron star mergers, causes ripples in the curvature of space-time due to a changing gravitational field. Such distortions, called gravitational waves, propagate at the speed of light and encode information about the events which produced them.

The passing of gravitational waves causes space to be stretched in one direction while simultaneously being squeezed in the perpendicular direction. The space-time strain, or change in length divided by length, induced by these waves can be up to ten thousand times smaller than the diameter of a proton. The detection of such perturbations in space time requires the use of a network of extremely sensitive laser interferometers, which acts as a transducer that translates the changes in strain produced by a gravitational wave into a signal which can be measured. In the United States, LIGO consists of two such detectors, one located in Hanford, Washington and the other in Livingston, Louisiana. These detectors are sophisticated versions of the Michelson interferometer, which splits laser light into two beams and sends the light down two perpendicular arms to be bounced off of optics and later recombined. The passing of a gravitational wave will change the relative lengths of the two arms, altering the time it takes the laser light to travel to the end of each arm and back. This difference in travel time between arms will cause the light to be out of phase when recombined, producing an interference pattern that follows the induced space-time strain [1].

Because gravitational waves produce minuscule levels of strain, to the order of 10^{-21} relative change in length, the interferometers must be incredibly sensitive to changes in length. However, with this sensitivity, the detectors are greatly affected by ground motion, storms, lightning strikes, and other forms of seismic noise which cannot be prevented. During times of elevated seismic noise, the effective visibility of the detectors is inhibited, and the detectors experience a reduction of sensitivity to gravitational waves. In addition, it is possible for noise to produce output that mimics the appearance of a gravitational wave. This makes it difficult to distinguish between actual instances of gravitational waves and otherwise insignificant noise events [2]. However, many sources of noise are known, and there are several ways to lessen their effects.

Inhibiting the effects of noise is achieved through the implementation of active and passive isolation. Passive isolation stages mitigate contact with the terrestrial environment, passively reducing the effects of seismic noise. This includes a vacuum chamber to enclose the instrumentation, as well as a quadruple pendulum test mass suspension system to suspend the optics at either end of the arms [3]. Active isolation uses information from the environment to actively combat the effects of noise. Within the vacuum tanks, this includes relative position sensors and seismometers, which measure the six degrees of freedom of the optics; this information is used in conjunction with feedback control loops in order to apply forces to the test masses opposing unwanted motion. Both types of isolation increase the range of which the instrument can see into the universe by reducing unwanted motion of the optics [3].

Though the use of such isolation has minimized the effects of noise on the detectors, we still observe complicated non-linear effects in the interferometer data [2]. Thus, it is important to

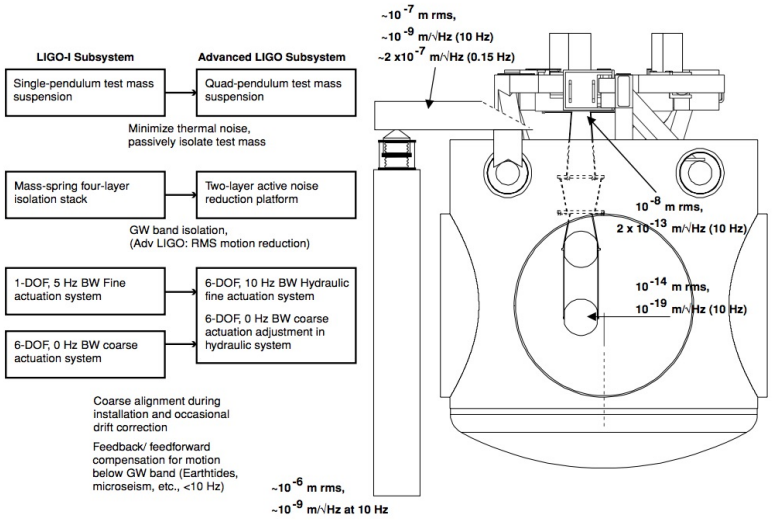

Figure 1: This figure depicts the active and passive isolation of LIGO and Advanced LIGO optics. [3]

evaluate the output of the interferometers during times of elevated seismic noise in order to better understand and predict the output data during times of elevated noise in the future.

2 Motivation

Despite the abilities of the isolation to mitigate the effects of seismic noise on the detectors, there are technological limits we must face when analyzing data. There exist times of elevated seismic noise when the active isolation cannot maintain a sufficient level of control over the test masses. During these times, the test masses are moving too much, and the detectors are thrown out of lock.

The motivation for this project however, comes from times of elevated seismic noise where the detectors remain locked and continue to take viable data. The elevated level of seismic noise affects the sensitivity of the detectors into the universe. We are mostly interested in quantifying this visibility of the detectors during these times as well as analyzing changes in sensitivity to gravitational waves over time.

Previous research in this area includes characterizing visibility of LIGO over five day spans. This is done by averaging the detector sensitivity of five days of coincident data between the Livingston and Hanford sites. Although this provides some level of insight into detector performance, a method in which smaller spans of time are considered would allow for more specific evaluations. Thus, we aim to modify the pre-existing sensitivity characterization method to assess detector performance over twenty-minute and ten-minute time-scales.

In addition, we aimed to analyze the behavior of the instrumentation during times of elevated seismic noise in order to more fully understand the resulting responses of the actively controlled optic cavities. Specifically, we aimed to characterize the effects of ground motion on the actively isolated platforms supporting the interferometer optics, as well as the response of the controlled interferometer cavities.

3 Overall Approach

Our first step in this project was to identify periods of elevated seismic noise, specifically increases in Earthquake band ground motion at frequencies of $0.03\text{Hz} - 0.1\text{Hz}$. To do this, we examined the ground motion at the detector sites during LIGO's second observing run and selected specific times during which it was likely to observe the effects of seismic noise in the gravitational wave strain output data.

We used PyCBC, a Python software package that uses matched filtering to identify modeled

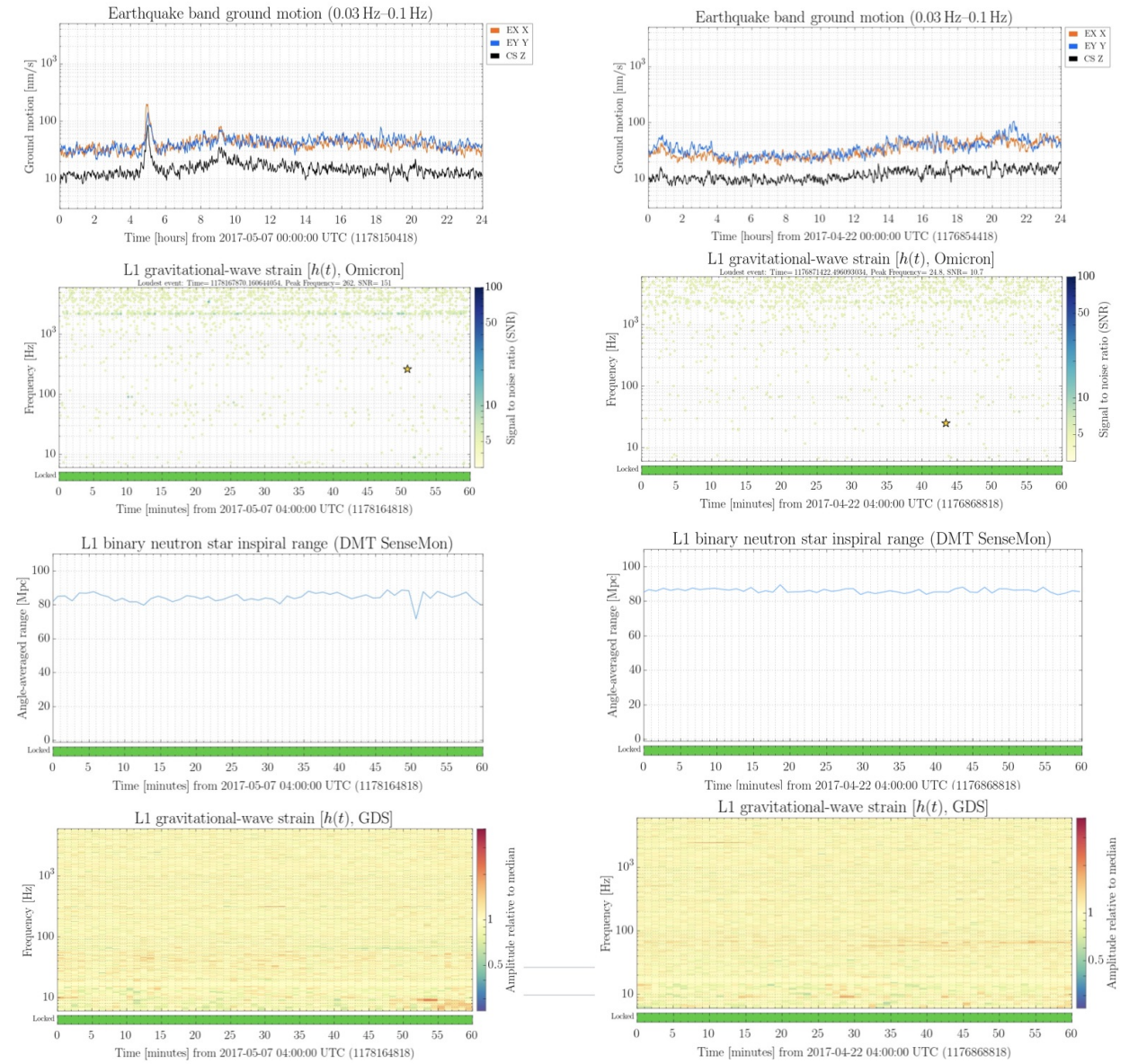

Figure 2: This figure depicts, from top to bottom, the earthquake band ground motion, glitch level, inspiral range, and gravitational wave strain of the Livingston observatory on May 7th, 2017 (left) and April 22nd, 2017 (right).

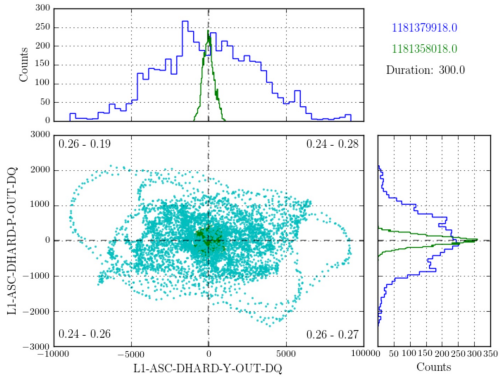

Figure 3: Phase-Space plot of the Livingston, Louisiana site on June 13th, 2017 at 9:05am.

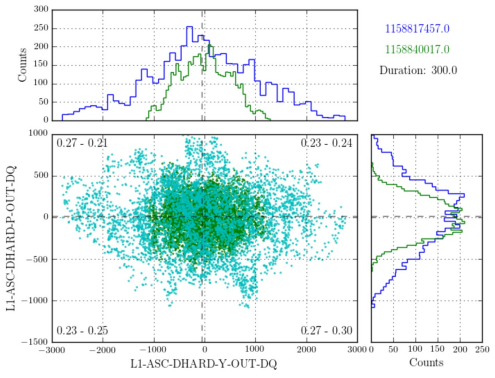

Figure 4: Phase-Space plot of the Livingston, Louisiana site on September 25th, 2016 at 5:44am.

compact binary coalescences, or CBCs, in this noisy data [4, 5], in order to evaluate the impact of the excess ground motion on searches for gravitational waves from compact binary sources. For this we used the output of completed PyCBC searches from the second observing run.

We used this procedure to study several instances of elevated ground motion in order to evaluate the long term behavior of the detectors and build a statistical distribution of results that can be used to predict future interferometer performance and behavior in response to elevated ground motion.

Lastly, we evaluated the performance of any proposed veto method targeting the characterized ground motion by measuring the difference in observed searchable volume-time using the PyCBC pipeline [4, 5].

4 Visualizing Movement of the Optics

We began the data analysis aspect of the project by identifying six total instances of significant earthquake band ground motion, above $200nm/s$ but not exceeding $700nm/s$, at either the Livingston or Hanford site where the associated detector remained locked. The range of ground motion was crucial in determining which times to use. Any motion less than $200nm/s$ did not produce obvious changes in output data, thus glitch level, inspiral range, and gravitational wave strain levels were consistent with those of seismically quiet times. For example, Figure 2 depicts the output of the Livingston detector on May 7th, 2017 compared to April 22nd, 2017. When looking at the Earthquake band ground motion of May 7th, we observe a small spike in ground motion, peaking at around $100nm/s$. Yet, there is no clear difference in the detector output which seems to be caused by the elevated noise. Thus, after considering several instances of smaller ground motion peaks, from $100nm/s$ to $400nm/s$, we determined the threshold for significant ground motion to be around $200nm/s$. In addition, the detectors can only withstand a certain level of motion without being thrown out of lock mode. Any times exceeding $700nm/s$ earthquake band ground motion would render the information unusable, and the detector would not continue taking data. Thus, $700nm/s$ was the upper limit for the level of earthquake band ground motion that we considered.

Phase-space plots depicting the motion of the optics from the corresponding detector location were created for each of the selected times. For example, Figures 3 and 4 depict the differential hard alignment mode of the Livingston detector on June 13th, 2017 and September 25th, 2016 respectively. The teal points mark the pitch versus yaw of the optics during a time of elevated noise, whereas the green points mark the pitch versus yaw of the optics during a seismically quiet time. Visual comparison of such plots provide insight into the consistencies or lack thereof of hard mode motion during earthquakes.

We observed that, as predicted by our original hypothesis, the pitch and yaw of the optics deviate from their respective averages much more during times of earthquakes than during seismically quiet times. We can see this in the way that the teal points in Figures 3 and 4 trace out a much larger area than the green points, showing larger deviations in pitch and yaw during earthquakes.

Spectrograms and Omega-scans of the seismically elevated times were made to visualize the re-

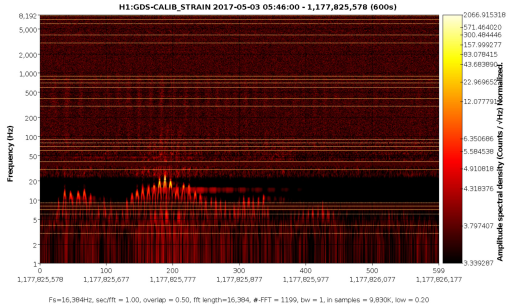

Figure 5: Spectrogram of the Hanford, Washington site on May 3rd, 2017 at 5:46am.

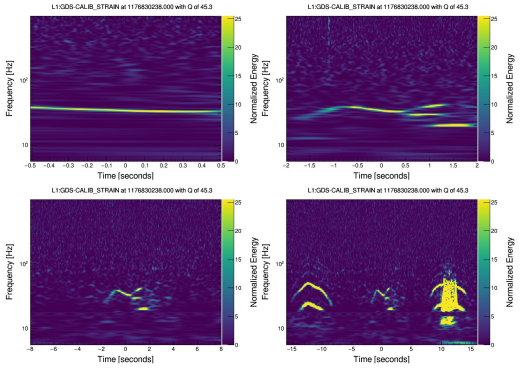

Figure 6: Omega Scan of the Livingston detector on April 21st, 2017

sulting glitches in time-frequency-energy space. Spectrograms are Fourier transform time-frequency representations, whereas Omega-scans are Q-transform based time-frequency representations. Omega-scans use sin waves called wavelets, short duration sine Gaussian bursts which model signals, to search for similar waveforms in the data.

Detector noise can cause recognizable patterns, for example scattering arches, in spectrograms and Omega-scans. This can be seen in Figures 5 and 6. Scattering arches are the effects of scattered light due to movement of the detectors. During earthquakes, the motion of the optics can send photons bouncing off the walls of the detector. Normally these photons are absorbed by the black baffles of the vacuum chambers, but occasionally they will bounce back into and recombine with the laser light. The light which was originally reflected can be slightly out of phase with and a different frequency than the laser beam, resulting in the arches visible in the plots.

Spectrograms and Omega-scans are used in visual comparison of the signals observed during the selected times from both detectors in order to more fully understand what could be causing a signal or glitch. These plots further enable us to characterize the detector output and behavior during times of elevated seismic noise.

5 Plotting Detector Sensitivity

One of the main focuses of our work is to characterize the change in sensitivity of the detectors due to elevated ground motion. Using the PyCBC sensitivity module, we developed a program to plot the sensitivity of the detectors to gravitational waves on a smaller time scale. We then used this plot to trend sensitivity changes during our selected times of elevated seismic noise.

When evaluating sensitivity of the LIGO detectors, we measure the sensitive volume or sensitive distance. There are several ways of doing this. One way detector sensitivity is currently evaluated is BNS inspiral range. This method assumes a $1.4M_{\odot}$-$1.4M_{\odot}$ BNS merger. Sensitive distance is then calculated by finding the average distance at which the system would need to be for its signal to be recovered with an SNR of 8, given the noise at that time. One problem with this method is its restriction to one type of merger.

We resolve this by calculating sensitive volume using injections. To do this, we add a large number of simulated signals with different physical parameters into the data. These parameters include distance from earth, masses and spins of the two bodies, orientation of the orbital plane, etc. The sensitive volume is determined by the number of recovered signals compared to the number of injected signals, as well as their physical parameters:[4]

$$V(F) = \int \epsilon(F; x; \Lambda)\phi(x; \Lambda)dxd\Lambda$$

where ϵ is the efficiency of detecting a signal with physical parameters Λ, in volume x, with false-alarm rate F, and $\phi(x; \Lambda)$ represents the distribution of signals within the universe. [4]

Previously, this method has been used to calculate detector sensitivity over five day spans of coincident data between the Livingston and Hanford detectors. However, it is difficult to determine short duration changes in sensitivity using this method, because it is unlikely for a fluctuation due

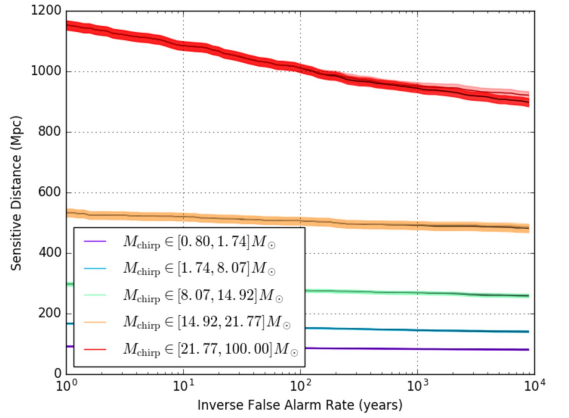

Figure 7: Sensitive Distance vs IFAR: binned by mchirp using pylal method.

to a short term elevation in seismic noise to alter the average sensitivity over five days. This is shown in Figure 7: rather than showing transient changes in sensitivity, this method shows us how sensitivity changes over longer time scales. The method that we developed to evaluate average sensitivity over shorter spans of time allows us to more accurately track changes in gravitational wave detection rates.

At first, our decision to bin the data into 20 minute chunks was determined because of our concern regarding error. If the error in our sensitivity measurement is too large, any changes in sensitivity would be indistinguishable from statistical fluctuations. For this reason, we needed to find a bin time where the errors were small enough that we could observe this. Because injections can either be found or missed, we use binomial error estimation to determine the error on our sensitivity calculation.

$$\hat{p} \pm \sqrt[2]{\frac{1}{n}\hat{p}(1-\hat{p})}$$

Here, we can see that binomial approximation is inversely proportional to the number of trials, n. Thus, the fewer trials which occur during the bin time, the less accurately we can measure the true sensitivity. Further, the shorter the bin time, the less total number of injections, and the larger the error.

Using 20 minute bins, the error bars were small enough to detect changes in sensitivity; however, when analyzing bin times that corresponded to peaks in earthquake band ground motion, we were not observing the level of sensitivity drop that we expected. For example, when plotting the sensitivity of June 24th, 2017 from 3:40pm to 5:00pm using twenty minute bins, we observed that the sensitivity for binary neutron star (BNS) systems for the bin time corresponding to an earthquake was higher than the median sensitivity for the total duration of an hour and twenty minutes. Along with this, the sensitivity to all other systems, although less than the median, was not significant compared to the fluctuations over the total duration.

We determined that this was due to two factors: the small fraction of seismically noisy time per bin, and the small number of total bins which resulted in an inaccurate median sensitivity. Most of the earthquakes we considered resulted in peak levels of elevated seismic noise lasting around five minutes. When using 20 minute bin times, these five minutes of lower sensitivity were averaged with fifteen minutes of normal levels of sensitivity. Thus, it is difficult to distinguish a significant dip. Along with this, the total duration of an hour and twenty minutes proved to be too short of a time, and it seemed that the concentration of seismically noisy time had too great of an impact on the median sensitivity, making it even less likely to distinguish a change in sensitivity during the earthquake peak.

This is resolved by binning the data into ten minute time scales and plotting the data over longer total durations. We can see the results of this in Figure 8, where the seventh bin corresponds to elevated seismic noise and we see a dip in sensitive distance below the median.

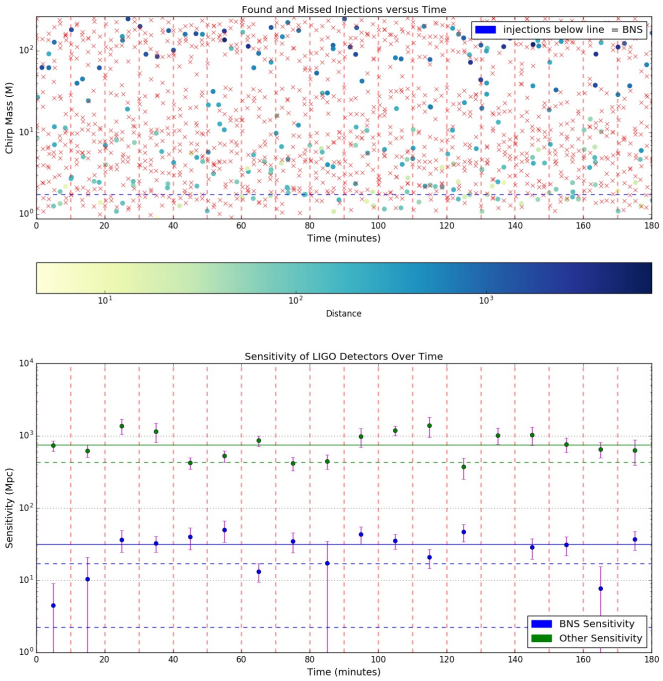

Figure 8: Sensitivity plots of June 24th, 2017 from 3:30pm to 6:30pm. The span of three hours is separated into ten minute bins. The seventh bin corresponds to a peak in elevated seismic noise.

6 Analyzing Sensitivity Over Time

Gravitational waves differ depending on the system which emitted them. The most drastic difference of waves occurs between binary neutron star (BNS) systems and other systems such as neutron star black hole (NSBH) and binary black hole (BBH) systems. BNS systems are much lower in mass, thus they emit weaker gravitational waves, and the distance which we can see them is much shorter than other systems. In addition, BNS waveforms are longer duration and generally last 30-60 seconds from 20Hz onward, whereas waveforms from higher mass systems can be as short as 0.1 second from 20Hz onward. The length of BNS waveforms increases the chance that the waveform will overlap with a glitch. Thus the ability to detect gravitational waves emitted by a BNS system is different from the ability to detect gravitational waves from other systems. In order to accurately analyze the changes in sensitivity of the detector, we must take these differences into consideration. Chirp mass, which determines the evolution of a gravitational wave, is defined as:

$$\mathcal{M} = \frac{(m_1 m_2)^{3/5}}{(m_1 + m_2)^{1/5}}$$

For our purposes, we consider $1.74 M_\odot$ to be the upper limit of the chirp mass for BNS systems.

Figure 8 depicts one of the sensitivity plots created for June 24th, 2017. The top plot shows found and missed injections per bin for the total three hour duration. Here we can visualize the difference between recovery of BNS waveform and other waveform injections. The bottom plot shows the sensitive distance of the detectors over time. A transient burst of about 300nm/s earthquake band ground motion peaked at 16:32:00 UTC, corresponding to the seventh bin on the plot.

We observe that the sensitivity of the detector to BNS waveforms dips below BNS sensitive median sensitivity by about $2 * 10^1$, whereas sensitivity to other waveforms is higher than the sensitive median for other systems. We predict a decrease in sensitivity due to elevated noise, thus this result is unexpected. However, this increase in BBH sensitivity is within one standard deviation from the median, thus we hypothesize that this is due to statistical fluctuation and is not significant.

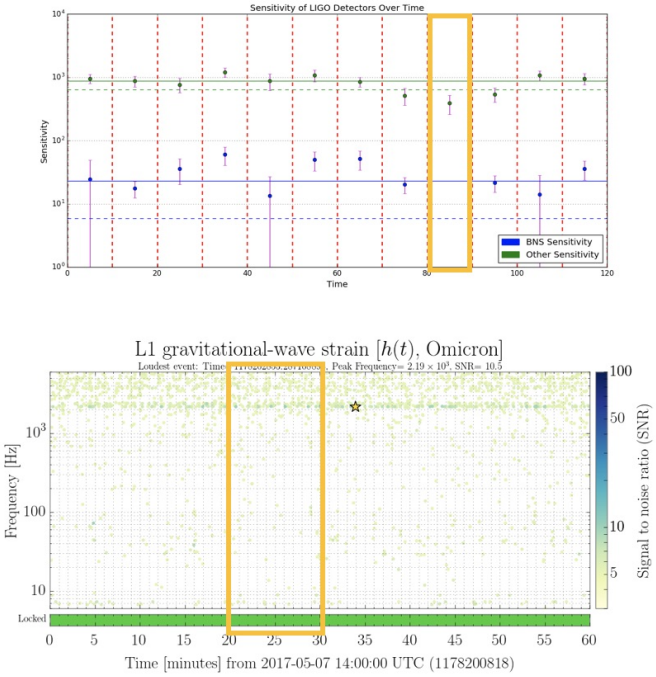

Figure 9: Sensitive distance (top) and measured gravitational wave strain (bottom) for LIGO Livingston on May 7th, 2017. The highlighted portions correspond to 2:20pm-2:30pm.

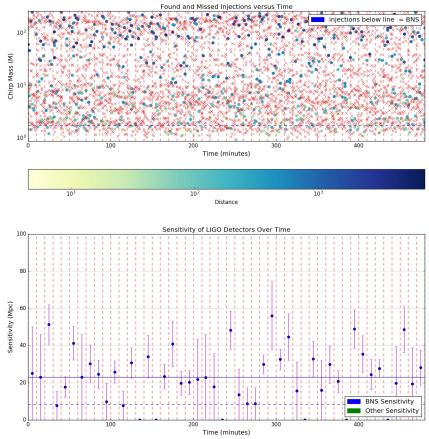

Figure 10: Found and missed injection plot (top) and sensitive distance plot (bottom) of April 21st, 2017 from 12:30pm to 8:30pm, calculated using the original injection file.

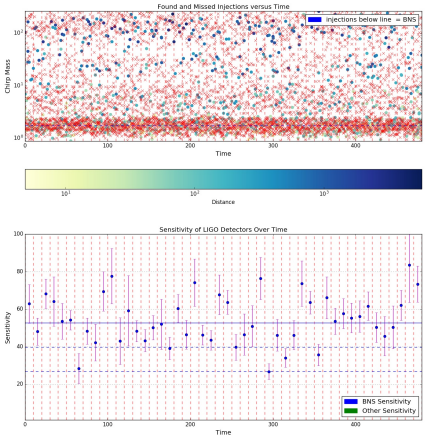

Figure 11: Found and missed injection plot (top) and sensitive distance plot (bottom) of April 21st, 2017 from 12:30pm to 8:30pm, calculated using extra injections.

7 Statistical Significance of 0Mpc Sensitivity

One observation we made when evaluating detector performance was an unusually high frequency of 0Mpc sensitive distance for BNS waveforms. In addition, many of the bins which reported 0Mpc sensitive distance corresponded to little or no elevated seismic noise, increased gravitational wave strain, or glitches. An example of this can be seen in Figure 9. We hypothesized that this is due to small number statistics.

When considering $1.74M_{\odot}$ as the cut off for BNS chirp mass, we observe an average of 8 BNS injections per bin. The fewer injections per bin, the more likely it is for the detector to miss all of the injections, and when this occurrs, we observe a 0Mpc sensitive distance for that ten minute time period. We can see this relationship in Figure 10, where the BNS injections are located below the dotted blue line on the top plot, and the corresponding sensitivity is located on the bottom plot.

To address this, we increased the total number of BNS injections for April 21st and reevaluated the sensitive distance, shown in Figure 11. With the increased BNS injections, not only do we observe 0 cases of 0Mpc sensitive distance, but we also observe a more accurate median and standard deviation. This enables us to more accurately identify significant dips in sensitivity.

8 Applying this method to April 21st, 2017

On April 21st, 2017 we observed a spike in earthquake band ground motion at the Livingston site at 17:17:00 UTC. Because ground motion was elevated to around 450nm/s, and both Hanford and Livingston detectors remain locked, this is an ideal test case for our method.

We observe the change in sensitive distance on the left side of Figure 12. The associated bins are highlighted in orange, and we observe a drop in sensitive distance to 26.7Mpc. This is two standard deviations below the median sensitive distance of 52.8Mpc, where the standard deviation of this 8 hour period is 12.9Mpc. We can further visualize the statistical significance of this drop by looking at the sensitive distance histogram for this 8 hour duration. The bin corresponding to the drop is an outlier, and we can conclude that this decrease is not due to standard statistical fluctuations.

In order to more fully understand what is affecting detector performance during this time we analyzed measured gravitational wave strain, BNS inspiral range, and fluctuations in time-frequency-energy space during this time. As seen in Figure 13, we observe scattering arches in both the Spectrogram and Omega scan of 17:17:00 UTC. We also observe a decrease in BNS inspiral range, an increase in glitches, and an elevated level of measured strain. Thus, we can conclude that our method of evaluating detector performance is sensitive to transient elevations in noise.

Further, we can conclude that, compared to BNS inspiral range, our method can more accurately determine sensitive distance at any given time. Figure 14 shows BNS inspiral range of the Livingston and Hanford detectors, where the highlighted portion roughly corresponds to the elevated level of seismic noise in question. Here, both detectors report around 60Mpc sensitive distance. However, when using our higher resolution method of 10-minute time scales, we conclude that sensitive distance during this time is around 26Mpc.

9 Difficulties Encountered

The first difficulty we faced during this project was finding times of significant increases in ground motion during which both detectors remained locked. For instance, we would often find times where one detector experienced an earthquake during which it remained locked, but the other detector was out of lock for an unrelated reason, such as maintenance or a larger earthquake. We would be unable to use this time, because we need coincident date between the two detectors to evaluate sensitivity.

Another difficulty we faced was distinguishing between which noise sources caused a decrease in sensitivity. There are many noise sources to consider, such as light scattering, anthropogenic noise, thermal noise, etc. Thus it is hard to determine if we are seeing a decrease in sensitive distance due to an increase in earthquake band ground motion, or another source.

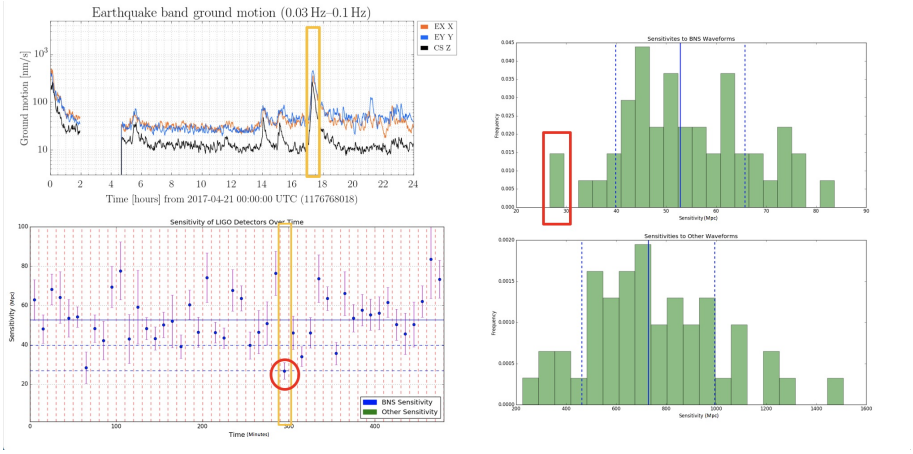

Figure 12: Earthquake band ground motion for April 21st, 2017 and the associated sensitive distance (left), and sensitive distance histogram for April 21st, 2017 (right).

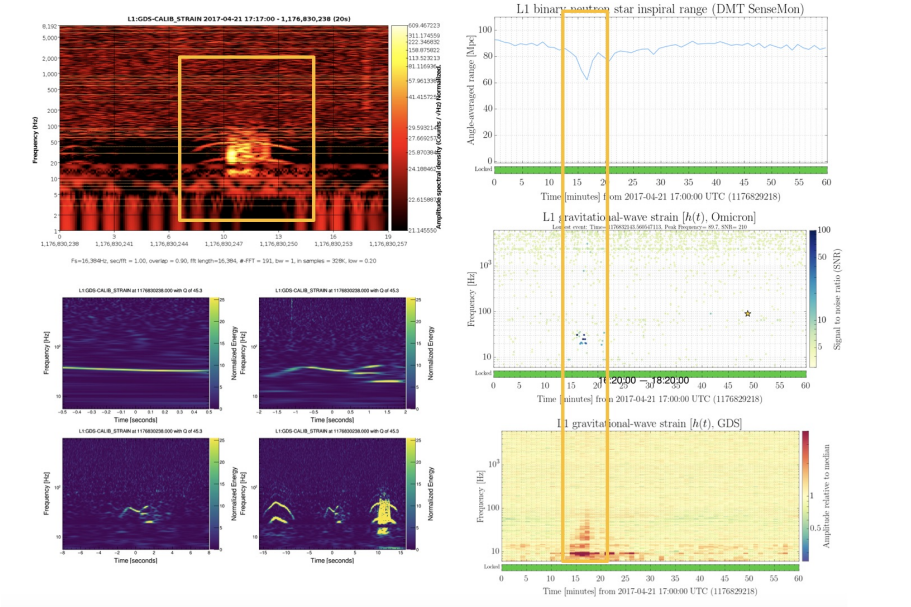

Figure 13: Spectrogram and Omega-scan (left), BNS inspiral range and measured gravitational wave strain (right) for the Livingston site on April 21st, 2017 at 17:17:00 UTC.

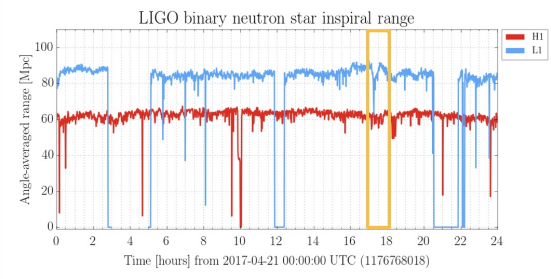

Figure 14: BNS inspiral range for Livingston and Hanford sites on April 21st, 2017.

10 Future Goals

First of all, we would like to increase the accuracy of our sensitivity calculations further. Thus far, we have increased the number of BNS injections, improving the accuracy, so we would like to apply this method to all chirp masses. In addition, we would like to separate the sensitive distances into more categories based on chirp mass, in order to get a more precise look at how sensitive distances to various systems change over time.

Another goal we have for the future is to investigate significant instances of 0Mpc sensitive distance. Perhaps work in this category can include developing a program to evaluate the significance of a 0Mpc sensitivity depending on number of missed injections versus total injections for that bin time. Further, ideally we would like to understand what is causing these significant dips in sensitivity, if not seismic noise. This research could introduce us to new sources of noise which we were unable to detect before.

Lastly, this method of evaluating sensitive distance is not restricted to times of elevated seismic noise. We would like to apply this method to times where other the detectors are subject to forms of noise, in order to more fully understand the different effects of noise.

References

[1] LIGO Scientific Collaboration, Virgo Collaboration, et al. Gw150914: The advanced ligo detectors in the era of first discoveries. *Phys. Rev. Lett.*, 116:131103, 2016.

[2] LIGO Scientific Collaboration, Virgo Collaboration, et al. Characterization of transient noise in advanced ligo relevant to gravitational wave signal gw150914. *CQG*, 33:134001, 2016.

[3] R. Abbott et al. Seismic isolation for advanced ligo. *IOPscience*, pages 1591 – 1597, 2002.

[4] Samantha A. Usman et al. The PyCBC search for gravitational waves from compact binary coalescence. *Class. Quant. Grav.*, 33(21):215004, 2016.

[5] Tito Dal Canton et al. Implementing a search for aligned-spin neutron star-black hole systems with advanced ground based gravitational wave detectors. *Phys. Rev.*, D90(8):082004, 2014.